

Exchange Biasing of the Ferromagnetic Semiconductor $\text{Ga}_{1-x}\text{Mn}_x\text{As}$

K. F. Eid, M. B. Stone, K. C. Ku, P. Schiffer and N. Samarth*

*Department of Physics and Materials Research Institute, Pennsylvania State University,
University Park, PA 16802*

ABSTRACT

We demonstrate the exchange coupling of a ferromagnetic semiconductor ($\text{Ga}_{1-x}\text{Mn}_x\text{As}$) with an epitaxially overgrown antiferromagnet (Mn). Unlike conventional exchange biased systems, the expected Néel temperature of the antiferromagnet ($T_N = 95$ K) is higher than the Curie temperature of the ferromagnet ($T_C = 52$ K). The resulting exchange bias manifests itself as a clear shift in the magnetization hysteresis loop when the heterostructure is cooled in the presence of an applied magnetic field and an enhancement of the coercive field, H_C . Both H_C and the exchange field, H_E , decrease monotonically with increasing temperature and vanish at the T_C of the ferromagnetic $\text{Ga}_{1-x}\text{Mn}_x\text{As}$ layer. Systematic thermal cycling studies identify a blocking temperature, $T_B = 46 \pm 4$ K.

* nsamarth@phys.psu.edu

Ferromagnetic semiconductors are currently the focus of extensive research, primarily due to their relevance in potential applications in semiconductor spintronics [1,2]. These hybrid materials offer new functionality because their carrier-mediated ferromagnetism can be manipulated by employing established techniques used in semiconductor technology (e.g. electrical gating and doping) [3]. A number of different “proof-of-concept” device geometries have been demonstrated using the “canonical” ferromagnetic semiconductor $\text{Ga}_{1-x}\text{Mn}_x\text{As}$, including magnetic tunnel junctions [4,5,6] spin light emitting diodes [7] and spin-tunable resonant tunnel diodes [8]. It is important in this context to develop a means of “exchange biasing” ferromagnetic semiconductors for device applications. This essentially entails exchange coupling the ferromagnetic semiconductor to a proximal antiferromagnet, and has been previously observed in ferromagnetic metals, intermetallic alloys, and oxides [9,10,11]. Although the exchange bias phenomenon was first observed almost half a century ago [12], a full understanding of the underlying physics is still under debate [9]. Exchange biasing of ferromagnetic layers in a spintronic device would have important beneficial effects such as increased stability and better field dependence than simple ferromagnetic/nonmagnetic multilayers; [13,14] exchange biasing of nanoparticles may also help to thwart superparamagnetic size effects [15], allowing for denser magnetic media.

The hallmark of an exchange biased system is a hysteresis loop which is not centered about zero magnetic field, but which is shifted either to positive or negative fields depending upon the orientation of the magnetic field applied while cooling the sample through the blocking temperature (T_B) of the antiferromagnetic layer. This is typically accompanied by an increase in the coercive field of the ferromagnet. We note

that the blocking temperature is usually lower than the Néel temperature (T_N) of the antiferromagnet. Further, in most conventional examples of exchange bias, T_B is lower than the Curie temperature (T_C) of the ferromagnet. Ferromagnetic semiconductors such as $\text{Ga}_{1-x}\text{Mn}_x\text{As}$ are of some interest in this context since T_C can be varied from liquid helium temperatures to around 150 K by varying sample parameters such as Mn concentration and sample thickness [16]; in principle, this may allow systematic studies of exchange biasing in a given ferromagnetic material over regimes where T_B can either lie above or below T_C .

We are aware of only one reported attempt at achieving an exchange bias in a III-V ferromagnetic semiconductor, using MnTe as the proximal antiferromagnet [17]. In that experiment, although the ferromagnetic semiconductor showed an increased coercive field at low temperatures, there was no conclusive evidence for an exchange coupling between the ferromagnetic semiconductor ($\text{Ga}_{1-x}\text{Mn}_x\text{As}$) and the overgrown antiferromagnet (MnTe). In this Letter, we demonstrate unambiguous exchange bias in a $\text{Ga}_{1-x}\text{Mn}_x\text{As}$ epilayer on which a thin layer of Mn has been deposited. While our experiments show clear evidence that such ferromagnetic semiconductors can indeed be exchange-biased, obtaining a routine and reproducible growth protocol to achieve such exchange-biasing will require further investigation of the details of the epitaxial growth process.

The samples studied in this work are grown on (001) semi-insulating, epi-ready GaAs substrates using low temperature molecular beam epitaxy. After thermal desorption of the oxide layer, a buffer is first deposited (comprised of a high temperature GaAs layer grown under standard conditions), followed by a low temperature GaAs layer grown at

250 °C. The magnetically active region of the sample is composed of a 10 nm thick ferromagnetic semiconductor $\text{Ga}_{1-x}\text{Mn}_x\text{As}$ layer ($x = 0.08$), capped with a thin (~ 4 nm) AFM Mn layer. We note that after the growth of the $\text{Ga}_{1-x}\text{Mn}_x\text{As}$ layer, the semiconductor wafer is removed from the growth chamber into a buffer chamber (also under ultrahigh vacuum) and the As cell is cooled down to room temperature. Once the As background pressure in the growth chamber is at an acceptable level, the substrate is reintroduced into the growth chamber, and the Mn capping layer is grown at room temperature. In another growth scheme, the sample is transferred in vacuum to an adjacent As-free growth chamber for the Mn capping. Successfully exchange-biased samples have been obtained using both schemes. These precautions are essential to avoid the formation of ferromagnetic MnAs during the growth of the capping layer.

The epitaxial growth is monitored by *in-situ* reflection high energy electron diffraction (RHEED) at 12 keV. During growth, the $\text{Ga}_{1-x}\text{Mn}_x\text{As}$ shows a clear reconstructed (1×2) RHEED pattern, while the Mn shows a weaker, yet streaky and unreconstructed pattern whose symmetry is suggestive of the stabilization of a cubic phase of Mn. The thickness of the $\text{Ga}_{1-x}\text{Mn}_x\text{As}$ layer is calculated from RHEED oscillations, while the thickness of the Mn overlayer is estimated from RHEED oscillations of MnAs whose growth rate is mainly determined by the sticking coefficient of Mn. The Mn concentration in the ferromagnetic layer is estimated at $x \sim 0.08$, based upon a calibration previously performed as a function of the Mn cell temperature ($T = 785$ °C) [18]. Magnetization measurements are performed using a commercial SQUID magnetometer, where samples are either field cooled or zero field cooled from room temperature to the measuring temperature in a finite or zero magnetic field respectively.

The antiferromagnet deposited on the ferromagnetic $\text{Ga}_{1-x}\text{Mn}_x\text{As}$ epilayer in the MBE chamber is nominally pure Mn (the source purity is 4N), and is expected to have a Néel temperature $T_N \approx 95$ K and a blocking temperature $T_B \approx 50$ K [9]. However, because Mn is highly reactive, we cannot rule out the possibility that the Mn layer is either oxidized upon removal from the growth chamber forming antiferromagnetic regions of MnO ($T_N \approx 150$ K) or that it has reacted with a near-surface region of $\text{Ga}_{1-x}\text{Mn}_x\text{As}$ forming regions of Mn_2As ($T_N \approx 573$ K) [19, 20]. We note that we have observed little change in the magnetization measurements over the course of six months, suggesting that if such a reaction has occurred, it may have affected the entire thickness of the Mn layer at the time of the first measurement. At present, due to the very limited thickness of the Mn layer, we do not have additional structural or compositional measurements that can definitively identify the specific nature of the overgrown Mn layer. Nonetheless, as we demonstrate, the evidence for exchange biasing by the top layer is quite unambiguous, and is consistent with either Mn or MnO as the biasing antiferromagnet.

Figures 1(a) and 1(b) depict two hysteresis loops for a $\text{Ga}_{1-x}\text{Mn}_x\text{As}/\text{Mn}$ heterostructure, measured at $T = 10$ K after cooling the sample in a magnetic field of $H = \pm 2500$ Oe. The “horizontal” offset of the hysteresis loops from the origin in a direction opposite to that of the cooling field is a clear signature of an exchange coupling with the overgrown antiferromagnet. Control measurements are used to rule out extrinsic effects: Fig. 1 (c) shows that cooling the sample in zero magnetic field results in no exchange bias, while Fig. 1 (d) the exchange bias shift is absent in a sample of similar thickness and grown under identical conditions, but without the antiferromagnetic overlayer. There is also a notable increase of the coercive field for the Mn-capped sample compared to

typical values for uncapped samples (see Figure 1(d)) [21], which is consistent with the expected effects of exchange biasing [9]. This is also consistent with the reported enhancement of the coercivity of $\text{Ga}_{1-x}\text{Mn}_x\text{As}$ due to the proximity of an antiferromagnetic semiconductor, which was, however, not accompanied by a shift of the hysteresis loop [17].

Figures 2(a) and (b) compare the field cooled hysteresis loops at two different temperatures (5 K and 30 K, respectively). In these plots, the sample is cooled from $T > T_C$ to the measuring temperature in a field of $H = 2500$ Oe. As the temperature is increased, the hysteresis loops become narrower, and their centers move closer to the origin. As the temperature approaches T_C , the hysteresis loop collapses into a single non-hysteretic curve of zero coercivity (not shown), indicating that the $\text{Ga}_{1-x}\text{Mn}_x\text{As}$ layer has become paramagnetic.

Figure 2(c) summarizes the temperature dependence of the hysteresis loop parameters H_E and H_C , showing a monotonic decrease in both as a function of temperature. The temperature dependence of both H_E and H_C mirrors that of the magnetization, which is shown in Fig. 2(d), indicates the Curie temperature of the Mn capped $\text{Ga}_{1-x}\text{Mn}_x\text{As}$ layer to be $T_C = 55.1 \pm 0.2$ K. We note incidentally that the absence of any appreciable background magnetization beyond T_C in either of the samples measured demonstrates the absence of observable MnAs clusters or any ferromagnetism derived from the Mn capping layer; this is verified by carrying out magnetization measurements above the Curie temperature of MnAs (320 K) [22]. Furthermore, both the value of T_C and the magnitude of the saturation magnetization are similar for the uncapped and

capped samples, indicating that the Mn overlayer does not affect the ferromagnetic state of the $\text{Ga}_{1-x}\text{Mn}_x\text{As}$ layer except through the exchange biasing.

Figure 3 shows the dependence of the hysteresis loop parameters (H_E and H_C) on the magnitude of the cooling field. Interestingly, we find that cooling fields as small as $H = 25$ Oe produce a significant exchange bias, and both H_E and H_C vary only slightly with the magnitude of cooling field up to $H \gg H_E, H_C$. These data indicate that once the exchange bias has been established, it becomes insensitive to the magnitude of the cooling field.

The blocking temperature (T_B) of the antiferromagnetic layer is estimated using a systematic temperature cycling protocol. We first cool the sample from $T = 300$ K to $T = 10$ K in an external field $H = 100$ Oe, and we measure the hysteresis loop at 10 K to check for consistency. After that, we raise the sample temperature to a certain value, T_{Test} in zero field, apply a field of 20 Oe in a direction opposite to that of the original cooling field, and then cool the sample back to $T = 10$ K in the presence of this field. At this point, we measure a detailed hysteresis loop. If $T_{\text{Test}} > T_B$, the horizontal shift of this hysteresis loop should be opposite to that of the original loop measured after the initial cooling. On the other hand, if $T_{\text{Test}} < T_B$, the shift in the second hysteresis loop should be in the same direction as that of the initial loop since the bias direction is still “frozen in.” Based upon those measurements, we estimate $T_B = 46 \pm 4$ K.

Comparisons between our observations and studies of other exchange-biased systems reveal important differences. First, for the FC hysteresis loops at and beyond $T = T_C$, the magnetization passes through the $M=0, H=0$ even though the sample has been cooled in a magnetic field. This observation stands in contrast to earlier studies reported

in exchange biased ferromagnetic *metallic* alloys with $T_C < T_N$, where FC hysteresis loops still indicate bias effects even in the paramagnetic state of the ferromagnetic material [23]. Further, both H_E and H_C have a similar functionality to the temperature dependent magnetization, shown in Fig. 2(d). This monotonic temperature dependence of H_E and H_C is also different from the non-monotonic reported for systems with either $T_B < T_C$ [9] or $T_B > T_C$ [23]. We speculate that the different behavior in our samples could be due to the close values of T_C and T_B or due to the different nature of the exchange coupling between a ferromagnetic *semiconductor* and an antiferromagnet, since the ferromagnetic coupling involves much smaller Fermi wave vectors.

The data shown above are from a single sample, and we have observed exchange biasing in one other sample out of the ten total that were grown under similar conditions. The difficulty in reproducing the results suggests that there may be rich behavior in the microscopic details of the epitaxial growth, and suggests an avenue for further exploration since the nature of interfaces appears to be crucial to the physics of ferromagnetic semiconductors [24]. We also note that our experiments are currently limited to Mn and MnSe in the choice of the possible antiferromagnetic material due to the configuration of the growth chambers (MnSe overlayers have not yielded any signs of exchange coupling with $\text{Ga}_{1-x}\text{Mn}_x\text{As}$). More standard antiferromagnets like FeMn and NiMn may be better choices for exchange biasing of this material, and we hope that the demonstration of feasibility in this work provides motivation for such experiments.

This research has been supported by grant numbers ONR N00014-99-1-0071 and -0716, DARPA/ONR N00014-99-1093 and -00-1-0951, and NSF DMR 01-01318. We thank C. Palmstrom and J. Bass for useful discussions.

Figure 1. Hysteresis loops of a $\text{Ga}_{1-x}\text{Mn}_x\text{As}$ ($t = 15$ nm)/ Mn ($t \sim 4$ nm) heterostructure measured at $T = 10$ K, after cooling in the presence of different magnetic fields: (a) $H = 2500$ Oe, (b) $H = -2500$ Oe and (c) $H = 0$. In (d), we show the hysteresis loop measured at $T = 10$ K for an uncapped $\text{Ga}_{1-x}\text{Mn}_x\text{As}$ ($t = 15$ nm) control sample, after field cooling in $H = 1000$ Oe. The diamagnetic and/or paramagnetic background has been subtracted off from these (and all subsequently presented) hysteresis loops.

Figure 2. Panels (a) – (c) provide a summary of the temperature dependence of the hysteresis loops and the hysteresis loop parameters for the sample described in Fig. 1. The hysteresis loop at any given temperature is measured after cooling the sample from $T = 100$ K to that temperature in a field $H = 2500$ Oe. Panels (a) and (b) show the field cooled hysteresis loop at $T = 5$ K and $T = 30$ K, respectively. Panel (c) shows the temperature dependence of the exchange field, $H_E = |(H_{C-} + H_{C+})/2|$, and the coercive field, $H_C = |(H_{C-} - H_{C+})/2|$ for $T < T_N$. The inset panel (d) shows the temperature dependent magnetization at $H = 20$ Oe, after field cooling in $H = 10$ kOe.

Figure 3. Hysteresis loop parameters at $T = 10$ K, as a function of the cooling field for the sample described in Fig. 1. Measurements are taken after cooling from $T = 100$ K to $T = 10$ K in the respective magnetic fields. Note that field axis is split at $H = 1.1$ kOe and is depicted on different scales for magnetic fields less than or greater than this value.

References

1. H. Ohno in *Semiconductor Spintronics and Quantum Computation*, eds. D. D. Awschalom, D. Loss & N. Samarth, (Springer-Verlag, Berlin, 2002), p.1.
2. S. A. Wolf, D. D. Awschalom, R. A. Buhrman, J. M. Daughton, S. von Molnar, M. L. Roukes, A. Y. Chtchelkanova, and D. M. Treger, *Science* **294**, 1488 (2001).
3. H. Ohno, A. Shen, F. Matsukura, A. Oiwa, A. Endo, S. Katsumoto, and Y. Iye, *Appl. Phys. Lett.* **69**, 363 (1996)
4. M. Tanaka and Y. Higo, *Phys. Rev. Lett.* **87**, 026602 (2001).
5. S. H. Chun, S. J. Potashnik, K. C. Ku, P. Schiffer, and N. Samarth, *Phys. Rev. B* **66**, 100408(R) (2002).
6. R. Mattana, J.-M. George, H. Jaffres, F. Nguyen Van Dau, and A. Fert, B. Lepage, A. Guivarc'h, and G. Jezequel, *Phys. Rev. Lett.* **90**, 166601(2003).
7. Y. Ohno, D. K. Young, B. Beschoten, F. Matsukura, H. Ohno, and D. D. Awschalom, *Nature* **402**, 790 (1999).
8. H. Ohno, N. Akiba, F. Matsukura, A. Shen, K. Ohtani, and Y. Ohno, *Appl. Phys Lett.* **73**, 363 (1998).
9. J. Nogués and I. Schuller, *J. Magn. Magn. Mater.* **192**, 203 (1999).
10. X. W. Wu and C. L. Chien, *Phys. Rev. Lett.* **81**, 2795 (1998).
11. P.J. van der Zaag, R.M. Wolf, A.R. Ball, C. Bordel, L.F. Feiner, and R. Jungblut, *J. Magn. Magn. Mater.* **148**, 346 (1995).
12. W. H. Meiklejohn and C.P. Bean, *Phys. Rev.* **102**, 1413 (1956).
13. L. Thomas, M. S. Samant, and S. S. Parkin, *Phys. Rev. Lett.* **84**, 1816 (2000).
14. K. Nagasaka, Y. Seyama, L. Varga, Y. Shimizu, and A. Tanaka, *J. Appl. Phys.* **89**, 6943 (2001).
15. V. Skumryev, S. Stoyanov, Y. Zhang, G. Hadjipanayis, D. Givord, and J. Nogués, *Nature* **423**, 850 (2003).
16. K. C. Ku, S. J. Potashnik, R. F. Wang, S. H. Chun, P. Schiffer, N. Samarth, M. J. Seong, A. Mascarenhas, E. Johnston-Halperin, R. C. Myers, A. C. Gossard, and D. D. Awschalom, *Appl. Phys. Lett.* **82**, 2302 (2003).
17. J. K. Furdyna, X. Liu, Y. Sasaki, S. J. Potashnik and P. Schiffer, *J. Appl. Phys.* **91**, 7490 (2002).
18. S. J. Potashnik, K.C. Ku, R. Mahendiran, S.H. Chun, R.F. Wang, N. Samarth, and P. Schiffer, *Phys. Rev. B* **66**, 012408 (2002).
19. W. Van Roy, H. Akinaga, S. Miyanishi, and K. Tanaka, and L. H. Kuo, *Appl. Phys. Lett.* **69**, 711 (1996).
20. J. L. Hilton, B. D. Schultz, S. McKernan, and C. J. Palmstrøm (unpublished).
21. S. J. Potashnik, K. C. Ku, R. F. Wang, M. B. Stone, N. Samarth, P. Schiffer, and S. H. Chun, *Journal of Applied Physics* **93** 6784 (2003).
22. S. Andrieu, H. Fischer, E. Foy, P. Lefevre, M. Alnot, and M. Piecuch, *J. Magn. Magn. Mater.* **198-199**, 285 (1999).
23. J. Cai, K. Liu, and C. L. Chien, *Phys. Rev. B* **60**, 72 (1999).
24. M. B. Stone, K. C. Ku, S. J. Potashnik, B. Sheu, N. Samarth, and P. Schiffer, *Appl. Phys. Lett* **83**, 4568 (2003).

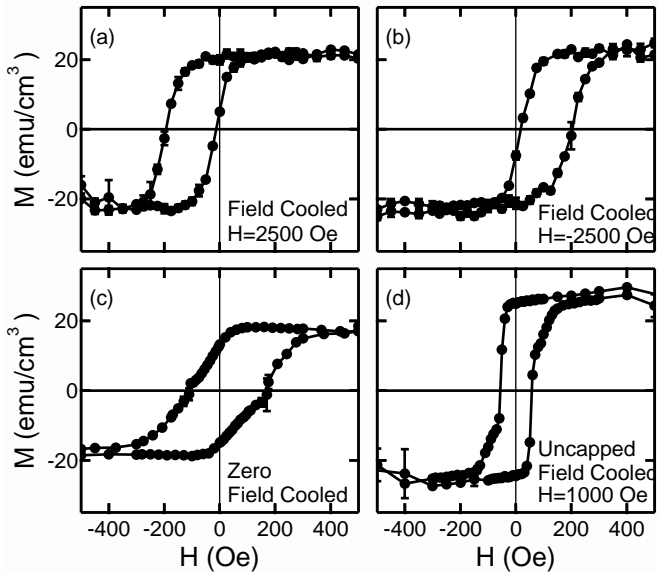


Figure 1, K. F. Eid *et al.*

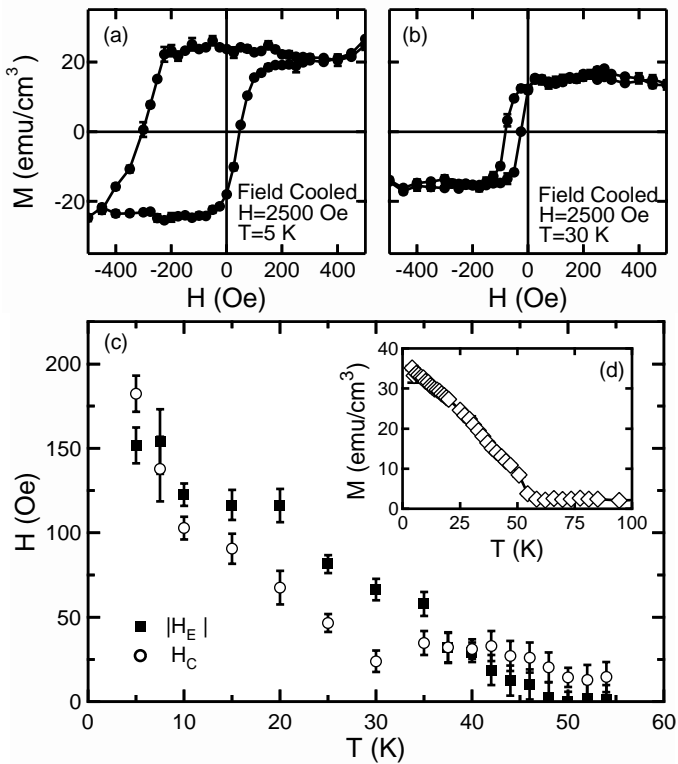


Figure 2, K. F. Eid *et al.*

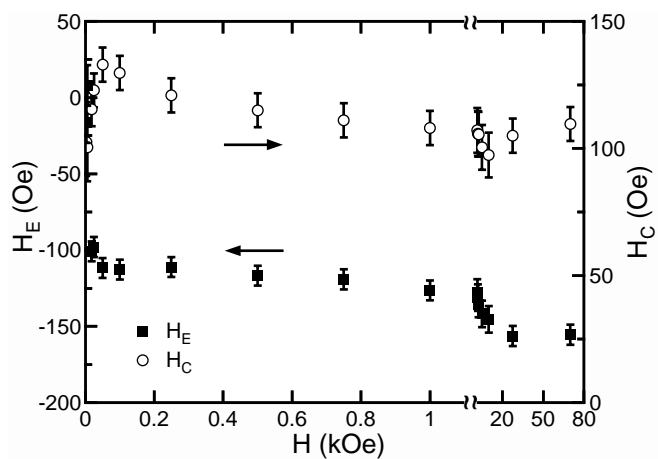


Figure 3, K. F. Eid *et al.*